analytical chemistry

Technical Note

pubs.acs.org/ac

Rapid Matrix-Assisted Laser Desorption/Ionization Time-of-Flight Mass Spectrometry Imaging with Scanning Desorption Laser Beam

Antonín Bednařík,[†,‡] Pavel Kuba,[§] Eugene Moskovets,[∥] Iva Tomalová,[†,‡] Pavel Krásenský,[‡] Pavel Houška,[§] and Jan Preisler*[,†,‡]

[†]Central European Institute of Technology (CEITEC), Masaryk University, 625 00 Brno, Czech Republic

[‡]Department of Chemistry, Faculty of Science, Masaryk University, Kamenice 5, 625 00, Brno, Czech Republic

[§]Faculty of Mechanical Engineering, Brno University of Technology, Technická 2896/2, 616 69 Brno, Czech Republic

[∥]MassTech, Inc. 6992 Columbia Gateway Drive, Suite No. 160, Columbia, Maryland 21046, United States

Supporting Information

ABSTRACT: Matrix-assisted laser desorption/ionization time-of-flight mass spectrometry (MALDI TOF MS) imaging of surfaces and tissues is a rapidly evolving technique having great potential in the field of biosciences. In earlier times, acquisition of a single high-resolution MS image could take days. Despite the recent introduction of high-repetition rate lasers to increase sample throughput of axial TOF MS instruments, obtaining a high-resolution image still requires a few hours. This paper shows that a substantial increase in the throughput of the TOF MS-based tissue imaging can be achieved by incorporating a mirror providing high-speed precision scanning of the laser beam along the sample surface. Equipped with the scanning mirror, a laboratory-built axial MALDI TOF MS instrument utilizing a 4-kHz UV laser recorded a 100 × 100 pixel MS image in ∼11 min using 100 laser shots per pixel. This is almost an order of magnitude faster when compared to a modern commercial instrument equipped with 1-kHz laser.

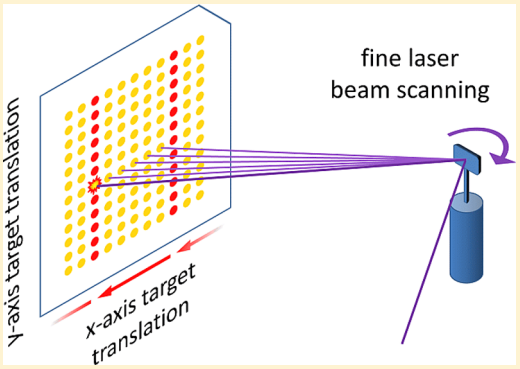

The matrix-assisted laser desorption/ionization mass spectrometry (MALDI MS) imaging of biological tissues emerged at the end of the last century[1] and has taken an influential place among imaging techniques during the past decade.[2,3] MS imaging of tissue samples is performed directly from a matrix-covered thin tissue slice and does not require labeling of the analytes, which presents a great advantage over fluorescence imaging or autoradiography.[4]

An important aspect for automation of the technique and its translation to the clinical practice is a high-throughput workflow. Axial TOF analyzers where the samples are analyzed in a high vacuum are predestined for high-throughput analysis due to (i) unsurpassed acquisition speed, orders of magnitude greater compared to other mass spectrometers (∼100 μs for a single laser shot spectrum for masses <3 000 Da); (ii) high resolving power (currently, >30 000 for peptides); and (iii) its ability to produce mass spectra of femtomole quantities of analytes over large m/z range in each laser shot.[5] Aside from the MS imaging throughput, which will be discussed below in the text, the total sample throughput is limited by the time necessary for sample preparation. The latter includes tissue cryosectioning, washing, drying, matrix application, as well as sample introduction into MS (pump down time). Yet, with a proper workflow organization, these restrictions will not affect the overall MS imaging throughput. For instance, sample preparation can be multiplexed and sample loading can be done in an express and automated manner using sample loading robots and sample storage chambers with controlled environments.[6]

A typical MALDI TOF MS imaging scan is performed in a rastering (target translation) mode. It comprises a series of MS signal acquisition events in a course of consecutive laser irradiation of multiple elementary spots (pixels) on a surface of matrix-covered tissue. In an elementary spectrum acquisition event, the laser performs a certain number of laser shots, all aimed at a single pixel, the individual MS spectra are recorded, averaged, and the data are sent to a PC for software processing and storage. At the end of individual pixel data acquisition, the laser is turned off and the MALDI plate with the sample is translated to a new position, then after the plate motion has ceased, the laser is turned on thus starting the signal acquisition from a new pixel. In this rastering mode, the fixed position of the laser spot with respect to the axis of the ion-optic system of the axial TOF mass spectrometer is selected to ensure stability of flight paths for desorbed ions from the area of laser spot on the MALDI plate to the ion detector thus keeping high the resolving power of the axial TOF-MS instrument.

Received: September 5, 2013
Accepted: December 23, 2013
Published: December 23, 2013

   dx.doi.org/10.1021/ac402823n | *Anal. Chem.* 2014, 86, 982−986

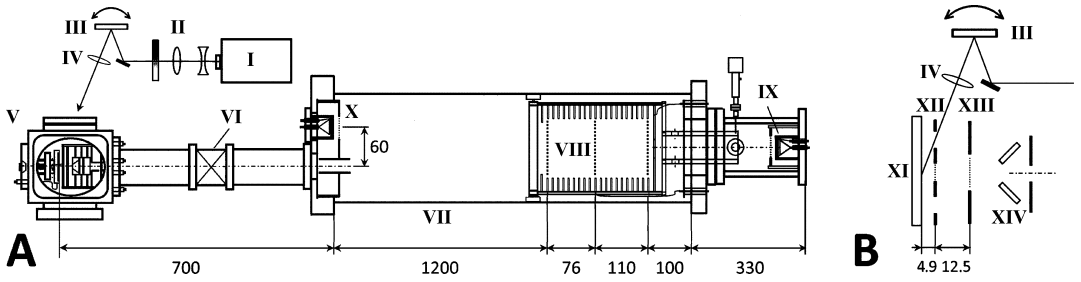

Figure 1. (A) Experimental arrangement (shown not in scale) of the laboratory-built MALDI TOF mass spectrometer with a fast scanning of the laser beam. (B) Detail of scanning from the side avoiding the ion source grids. (I) 355-nm Nd:YAG laser; (II) laser beam optics comprising the variable density filter and beam expander; (III) scanning mirror; (IV) focusing lens (focal length is 254 mm); (V) ion source with $X-Y$ moving stages and ion extraction/deflection optics; (VI) gate valve; (VII) flight tube; (VIII) dual-stage ion mirror; (IX, X) MCP detectors; (XI) MALDI target, the repeller; (XII) the extraction electrode; (XIII) the accelerating electrode; (XIV) set of mirrors.

Time t_{cycle} needed for recording one pixel in MS imaging can be expressed by the following equation:

$$t_{cycle} = t_{acq} + t_{proc} + t_{trans}$$

The total MS imaging time is then

$$t_{total} = nt_{cycle}$$

Acquisition time t_{acq} is the time necessary to record MS spectra from individual shots aimed at a single pixel, processing time t_{proc} is the time necessary for on-the-fly data processing (averaging) and storage, translation time t_{trans} is the time necessary to move the sample to a new position, and n is the number of pixels in the image. For a single MS image of a biological tissue, n can reach 100 000 or even more.

The early MALDI TOF imaging experiments were conducted using instruments equipped with nitrogen lasers operating at 2–20 Hz.[1,7,8] Acquisition time t_{acq} was the slowest step limiting the overall throughput of MS imaging. So, only a few pulses were usually fired at each pixel to attain reasonable throughput. MALDI MS throughput was increased by utilization of 355 nm Nd:YAG solid state lasers operating at kHz frequencies.[9] During the past decade, commercial MALDI TOF instruments with 200-Hz Nd:YAG lasers were gradually replaced by those equipped by 1-kHz and, finally, 5-kHz lasers.[4,10] Utilizing 10-kHz and higher repetition rate lasers may not be practical due to the upper limit (~150 μs) on flight times of heavier ions ($m/z \sim 5\,000$) in axial TOF MS instruments with high-resolving power.

With commercially available TOF MS instruments utilizing 5-kHz lasers, the acquisition time t_{acq} is no longer a limiting factor, the latter becomes determined by a combined contribution of t_{proc} and t_{trans}. Processing time t_{proc} usually ranges from tens to hundreds of milliseconds. In principle, it can be significantly reduced by using parallel data processing along with real-time spectrum averaging. Translation time t_{trans}, which can be 100 ms or more, varies considerably depending on the stage model, pixel-to-pixel distance, and the required positioning precision.

To increase MS imaging speed, continuous laser raster sampling has been introduced.[11] In this sampling mode, the laser fires continuously as the sample stage moves with a constant speed over the area of interest. This mode allows one to avoid spending time on wasteful stop-and-go plate travel events. A disadvantage of continuous scanning is the inevitable loss of spatial resolution due to mixing of ion signals from adjacent pixels: in this mode, the ion signal from the previous pixel is partially present in the signal from the next one. Time needed for the sample stage movements may also be reduced using an optical system for spatially dynamic patterning of the MALDI laser beam.[12] Another technique capable of boosting the throughput of the MALDI TOF MS imaging exploits the advantage brought by ion microscopy. In theory, the MALDI TOF MS system operating as the ion microscope can provide rapid MS mapping of large areas with high spatial resolution. Although current ion detectors used in ion microscopes suffer from saturation and low read-out rate, a remarkable progress in terms of acquiring a wider mass region with practical mass resolution has been reported.[13]

To reduce the bottleneck brought about by a large translation time t_{trans}, a novel sampling approach is presented in this paper which utilizes a new laser beam scanning mode. This approach is based on the use of an optical scanning system capable of fast and precise redirection of the laser beam across the stationary sample on a submillisecond scale. The laser scanning mode is especially advantageous when used together with high-repetition rate lasers, thus presenting a powerful alternative to the continuous raster sampling. In the laser scanning mode, possible over-sampling (burning the sample out) or overlap with neighboring pixels are avoided by firing a well-defined number of laser pulses at each pixel.

EXPERIMENTAL SECTION

Chemicals. Synthetic peptide, adrenocorticotropic hormone fragment 18-39 (ACTH), 2,5-dihydroxybenzoic acid (DHB) matrix, and trifluoroacetic acid (TFA) were purchased from Sigma-Aldrich (St. Louis, MO). Methanol was purchased from Scharlau Chemie S.A. (Barcelona, Spain). All chemicals were analytical-reagent grade.

Sample Preparation. For sample preparation, 40 mg of DHB matrix were dissolved in 1 mL of 80:20 (v/v) methanol/water solution containing 0.2% TFA. The matrix solution was mixed with 20 μM ACTH aqueous solution in the ratio 1:1 (v/v).

The mixture was deposited on the MALDI plate or the imaging glass slide (Bruker Daltonics, Bremen, Germany) using an airbrush GRAFO T1 (Harder & Steenbeck Airbrush, Norderstedt, Germany) with a 0.15 mm orifice. A volume of 200 μL of the matrix–peptide mixture was continuously sprayed on the plate from the distance of 8 cm through a 7 mm circular mask under a working pressure of 300 kPa.

Laboratory-Built Mass Spectrometer. The high-throughput axial MALDI TOF mass spectrometer was originally designed by Moskovets et al.[14] and modified in our laboratory (Figure 1A). The instrument was used in the positive mode; a detailed description of the instrument is in the Supporting Information.

dx.doi.org/10.1021/ac402823n | Anal. Chem. 2014, 86, 982–986

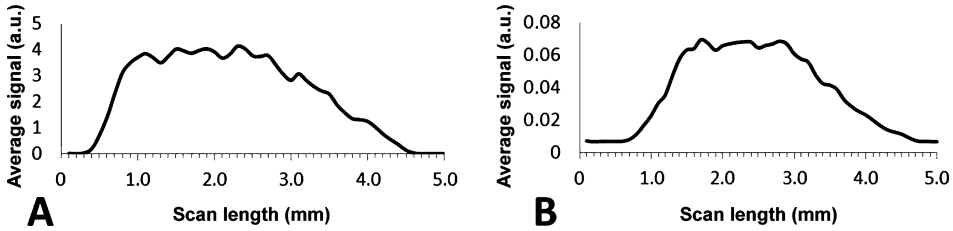

Figure 2. Signal (average over 2466.2 ± 1 m/z range) profile of the 5-mm laser beam scan across homogeneous sample layer of DHB with ACTH fragment 18-39 recorded at (A) linear and (B) reflector modes.

A 355-nm diode-pumped frequency-tripled Nd:YAG laser (DTL-374QT; Laser Compact, Moscow, Russia) operating at repetition rates from 200 Hz to 10 kHz served for desorption and ionization. The energy of the laser radiation was typically a 2.7 μJ/pulse at a 4-kHz repetition rate. Two high-vacuum compatible motorized linear stages (MM-3M-F stage for (X-) horizontal motion and MM-4M-Ex stage for (Y-) vertical motion, both from National Aperture, Salem, NH) moved the MALDI plate holder at speeds up to 5 mm/s, with a declared positioning accuracy of 3 μm. A high-speed 2 GS/s digitizer/averager (AP 200, Acqiris, Monroe, NY) was used for data acquisition and real-time averaging.

Fast Scanning Mirror with Precise Positioning. The unique feature of the instrument is a scanning mirror (6810P; Cambridge Technology, Lexington, MA) inserted into an optical pathway of the Nd:YAG laser. The voltage for a servo driver rotating the mirror around its vertical axis was generated by a NI myDAQ device (National Instruments, Austin, Texas). Redirecting the laser beam was accomplished by rotating the mirror at a small angle, this small-angle rotation of the mirror could be completed in only 400 μs, as stated by the manufacturer. The scanning mirror was also used to deflect the laser beam away from the target after the end of each single pixel or single mirror scan acquisition and thus served as an optical shutter. The ion source design of the laboratory-built mass spectrometer allowed the laser beam movement across the sample without an observable beam blocking in the range of about 10 mm.

Software. The operation of the laboratory-built instrument was conducted by using *DrobControl*, a program developed in *LabVIEW* programming environment. *DrobControl* was used for fast data acquisition, processing and storage in imzML format;[15] it controlled the movement of X- and Y-stages, and the rotation of scanning mirror. The stage translation (or mirror scanning) and data acquisition are consecutive tasks; data storage is concurrent with the target translation to the next pixel and subsequently to the next pixel data acquisition. Thus processing time t_{proc} is reduced to the minimum value required for command sending and data readout from the signal averager/digitizer.

Commercial Mass Spectrometer. AutoFlex Speed (Bruker) employing 1-kHz laser was used for comparison. The experiments on AutoFlex Speed were controlled by *FlexControl 3.3* and *FlexImaging 3.0* software, the system parameters (specified in the Supporting Information) were approximated to those of our laboratory-built instrument. Raw unreduced data (100 352 data points per spectrum, m/z range 500−4380) were acquired at 2 GS/s and stored in Bruker data format with minimal software processing, e.g., the baseline subtraction and spectra smoothing were turned off to maximize the imaging speed.

RESULTS AND DISCUSSION

Selection of Instrumental Arrangement. The ion images of the samples were acquired using a serpentine laser beam path pattern. Laser scanning mode imaging was initially performed with the laser beam aimed at a 20° angle, with respect to the MALDI target normal, passing through the centers of mesh electrodes in the ion source. In this arrangement, vertical lines with very low or no $[ACTH + H]^+$ signal intensities spaced 500 μm from each other were observed in the MS images (data not shown) which corresponds to the mesh specifications (mesh wires diameter 33.0−40.6 μm, the distance between the wires 508 μm).

Because of the large mesh-induced signal variation in images, the laser beam was aimed at a 75° angle, with respect to the MALDI target normal, thus bypassing both meshes (Figure 1B). Changing the laser beam incidence angle from 20 to 75° resulted in an ellipsoid laser focus (30 μm × 120 μm) profile on the target, determined by the microscopic inspection of the samples after laser desorption. No decrease in the ion signals was observed, which corroborates the early experiments with the laser incidence angle.[16] It is known that resolving power can be dependent on the laser incidence angle. The resolving power of our instrument remained at 15 000 in the reflector mode though a decrease of resolving power would probably be observable in instruments with higher resolving power.

The darker-strip artifacts were significantly reduced in the second arrangement. Only small periodical signal variations with 500-μm spacing and an amplitude of about 10% of the average ion signal were observed. The reason was partial blocking of the ion beam itself by the mesh wires. Because these small periodical fluctuations were reproducible for a given experimental setup, they were removed by a simple correction method as described below. The focused laser spot positioning repeatability was 5 μm, as calculated from the manufacturer's specifications and confirmed by the measurement of the coordinates of spots burnt in the homogeneous sublimated layer of DHB. Although certain changes in laser focus during the mirror scan could be expected, no measurable difference in the size of the laser spots burnt in the layer of DHB matrix was observed for the 1-mm wide scan due to the large focal length (254 mm) of the focusing lens. This setup was used in all further experiments.

Determination of Scan Range. The maximum laser beam scan range allowing the collection of MALDI spectra without a decrease in the ion signal intensity was determined in the both linear and reflector modes in the following experiment. MS images of narrow strips (5 mm × 1 mm, 50 × 10 pixels, i.e. 100 × 100 μm^2 pixel size) from a center of 7-mm sample spots were acquired in both target translation and laser scanning modes. As expected, the ACTH ion signal (m/z = 2466.2) disappeared at the edges of the 5-mm long laser beam scan, while no signal change was observed in the traditional target translation mode.

dx.doi.org/10.1021/ac402823n | *Anal. Chem.* 2014, 86, 982−986

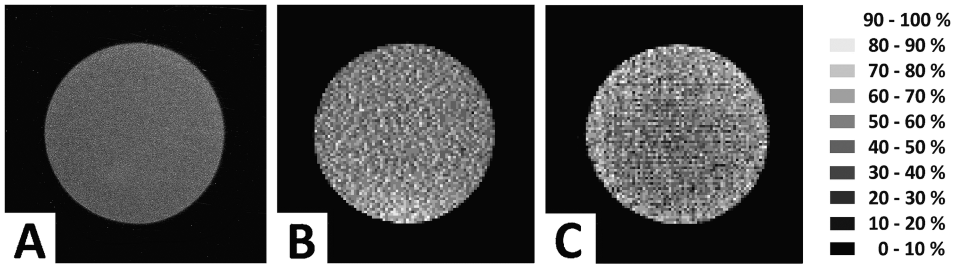

Figure 3. Images of the sprayed model sample: (A) photograph of the 7-mm circle model sample showing homogeneous airbrushed layer of DHB matrix. MS images of the model samples at m/z = 2466.2 ± 0.5 recorded in the reflector mode using (B) AutoFlex and (C) 4-kHz laboratory-built instrument with 1-mm laser beam scanning.

Table 1. Comparison of MS Imaging Time of 1-cm^2 Area (100 μm Resolution, 100 000 Pixels, 100 Laser Shots Per Pixel) With Autoflex Speed and the Laboratory-Built MS

device	sampling mode	f (kHz)	t_{trans} (ms/pixel)	t_{acq} (ms/pixel)	t_{proc} (ms/pixel)	t_{cycle} (ms/pixel)	t_{total} (min)
AutoFlex	translation only	1				465	77.50
lab-built MS	translation only	1	117	100	17.0	240	39.95
lab-built MS	1-mm laser scanning and translation	1	22	100	17.0	139	23.16
lab-built MS	translation only	4	117	26	17.0	160	26.70
lab-built MS	1-mm laser scanning and translation	4	22	26	17.5	66.5	11.08

The average signal from 50 columns was plotted versus the scan length and smoothed by averaging over 5 adjacent columns to show the trends in the signal intensity profile (Figure 2). The width of the plateau on the signal profile with intensity above 90% of the maximum signal was found to be 2.0 mm and 1.4 mm in linear and reflector modes, respectively. A smaller scanning range in the reflector mode reflected a more complex ion flight trajectory through the ion mirror and a smaller effective area of the ion detector used in the reflector mode compared to the one used in the linear mode.

Because of the large size of mesh covered apertures used in the ion source, resolving power should not deteriorate considerably during the laser beam travel across the sample.[9,16] No m/z shift was observed even for a 3-mm wide mirror scan and resolving power was found to be fixed at approximately 15 000 in the reflector mode.

The application of the scanning mode is not limited to samples with dimensions smaller than the mirror scan range. Larger sample areas can be imaged using a combined movement of the mirror and horizontal translation stage. The whole MS image is then stitched from the smaller mirror scanned segments. The stitched image acquisition is still much faster compared to the target translation mode because the number of stop-and-go translation steps can be diminished. Periodical signal variation, approximately $^1/_{10}$th of the average signal intensity, observed in the profile plateau was caused by the presence of meshes as described above. In the processed ion signal, this variation was practically eliminated using a simple correction method: the height of the ion signals obtained during a scan of the sample strip with a width defined by scan range was multiplied by a coefficient that compensated for the average decrease in the signal intensity. The correction coefficients were calculated for each of the pixel columns in the strip as the ratio of the average signal from the most intense column and the average signal from the respective column. The calculated correction coefficients were constant as long as the experimental setup and mirror settings remained unchanged. Operation in the laser scanning mode did not have a significant impact on the S/N ratio which stayed constant within the scan.

MALDI MS Imaging Acquisition Time. The total time necessary to accomplish MS imaging of the model sample was recorded for target translation and laser scanning modes using the laboratory-built instrument and compared to the performance of the commercial TOF mass spectrometer (AutoFlex Speed). The size and parameters of the recorded images were the same: 1-cm^2 square was divided into 10 000 pixels, which gave 100-μm spacing between the pixel centers; the MS spectrum recorded for each individual pixel was an average of 100 spectra and contained 100 000 data points (0.5 ns time bins, 32-bit signal resolution). In the scanning mode, the laser beam scan range was set to a length of 1 mm. Multiple MS images of a 7-mm circle of ACTH-sprayed samples were recorded and reconstructed within the selected m/z integration interval of 2466.2 ± 0.5 Da (Figure 3). The total acquisition times for both MS instruments are summarized in the Table 1.

First, the total MS imaging time was determined using the target translation (rastering) mode for both instruments operating at the same laser repetition rate of 1 kHz. Imaging time was 39.95 min (4.17 pixel/s) and 77.50 min (2.15 pixel/s), for the laboratory-built and commercial instruments, respectively. Note that the image acquisition in the commercial instrument was completed 15 min after the end of physical scan due to the computer having to read huge data arrays. The reduction of MS image acquisition time in our instrument was achieved using parallel raw data processing/storage system combined with fine-tuning of speeds of both X- and Y-translation stages for 100-μm steps.

The MS image with the same specifications was recorded in the scanning mode with a 1-kHz laser frequency in 23.10 min (7.22 pixel/s), reducing the imaging time by 16.85 min compared to the translation (rastering) mode.

Full imaging speed in the laboratory-built instrument has been achieved by using the 4-kHz laser repetition rate: in the translation mode, the imaging time was reduced to 26.70 min (6.24 pixels/s) and in the scanning mode, it was reduced to 11.08 min (15.04 pixels/s). From the total imaging time of 11.08 min, a mere 3.67 min were spent on the vertical and horizontal stage translation between the stitched segments, 4.33 min were required for data acquisition, and approximately 2.92 min for

dx.doi.org/10.1021/ac402823n | Anal. Chem. 2014, 86, 982−986

sending commands and data processing/storage. Mirror rotation during the scans took approximately 10 s in total.

The quality of recorded MS images (Figure 3) was compared in terms of relative standard deviation (RSD) of the ACTH signal acquired from the central 50 × 45 pixels in the sprayed area. RSD was 18% for the images recorded using the commercial instrument operating at 1 kHz; RSD was 28% and 25% for the raw and the corrected images, respectively, when using the laboratory-built instrument at 4 kHz. To perform signal correction of images recorded using the laboratory-built instrument, the correction coefficients were calculated from 60 rows of the central 1-mm mirror-scanned strip. It should be noted that there may be many reasons for the differences in the RSD values obtained with the two instruments, such as the different target surface (glass slide vs polished target used in the laboratory-built instrument), different laser spot profiles, and different laser pulse energy. In any case, the signal stability of the laboratory-built instrument was found to be as good as that of the commercial instrument.

CONCLUSIONS

A high-throughput MS imaging method that utilizes an axial TOF mass spectrometer has been developed. The speeds for different imaging approaches were measured using an airbrush-deposited layer containing a matrix and a single peptide. The high scan rate has been achieved by combining a 4-kHz UV laser, concurrent data storage/processing system, and high-precision optical scanning system capable of redirecting the laser spot across a small distance on the sample plate in less than 0.5 ms. The sampling mode utilizing the high-speed motion of the laser spot was shown to significantly outperform translation (rastering) mode, thus decreasing the imaging time.

The choice of a relatively shallow angle of sample irradiation and recalculation of experimental data were essential to attain the necessary quality of the MS images, free of artifacts of the laboratory-built TOF-MS system. In our best arrangement and when scanning a homogeneous sample, the signal intensity variation was less than 10% for maximum scan widths of 2.0 mm and 1.4 mm in linear and reflector modes, respectively. To reduce this small mesh-induced perturbation of the ion signal, a simple mathematical correction of signal intensities was applied. Images of a sample with length exceeding the maximum scan width were obtained by stitching images of shorter segments which were recorded by combining vertical oscillations of the laser spot produced by the fast mirror and slower horizontal motion of the sample plate. Minor changes in beam position with respect to the optical axis of the ion acceleration system of our mass spectrometer did not affect the resolving power, mass calibration, or S/N ratio.

Employing laser beam scanning, image stitching of 1-mm long segments, and using a UV laser with 4-kHz repetition rate, the 1-cm^2 area of the sample containing 10 000 (100 × 100) pixels was imaged in approximately 11 min using 100 laser shots per pixel.

In the future, gridless ion optics and a laser beam that hits the target surface almost orthogonally will be utilized to provide an unimpeded passage of both the laser beam and ions from the ion source and to create a circular laser spot with a top-hat intensity distribution on the target thus providing homogeneous sample illumination. This, together with the employment of a shorter-focal length lens, will significantly improve imaging resolution.

ASSOCIATED CONTENT

Supporting Information

Additional information as noted in text. This material is available free of charge via the Internet at http://pubs.acs.org.

AUTHOR INFORMATION

Corresponding Author

*E-mail: preisler@chemi.muni.cz.

Notes

The authors declare no competing financial interest.

ACKNOWLEDGMENTS

We gratefully acknowledge the financial support of the Czech Science Foundation (Grants GCP206/10/J012 and GAP206/12/0538), the project "CEITEC - Central European Institute of Technology" (Grant CZ.1.05/1.1.00/02.0068) from European Regional Development Fund and the program of "Employment of Newly Graduated Doctors of Science for Scientific Excellence" (Grant CZ.1.07/2.3.00/30.009) co-financed from the European Social Fund and the state budget of the Czech Republic. We also thank Barry L. Karger and Tomas Rejtar from Barnett Institute/Northeastern University for donating the initial instrument to us and putting it into operation and Lukáš Ertl from the Faculty of Mechanical Engineering, Brno University of Technology for early software development.

REFERENCES

(1) Caprioli, R. M.; Farmer, T. B.; Gile, J. *Anal. Chem.* **1997**, *69*, 4751−4760.
(2) van Hove, E. R. A.; Smith, D. F.; Heeren, R. M. A. *J. Chromatogr., A* **2010**, *1217*, 3946−3954.
(3) Watrous, J. D.; Alexandrov, T.; Dorrestein, P. C. *J. Mass Spectrom.* **2011**, *46*, 209−222.
(4) Khatib-Shahidi, S.; Andersson, M.; Herman, J. L.; Gillespie, T. A.; Caprioli, R. M. *Anal. Chem.* **2006**, *78*, 6448−6456.
(5) Vestal, M. L. *J. Am. Soc. Mass Spectrom.* **2011**, *22*, 953−959.
(6) McDonnell, L. A.; van Remoortere, A.; van Zeijl, R. J. M.; Dalebout, H.; Bladergroen, M. R.; Deelder, A. M. *J. Proteomics* **2010**, *73*, 1279−1282.
(7) Han, J.; Schey, K. L. *Invest. Ophthalmol. Vis. Sci.* **2006**, *47*, 2990−2996.
(8) Chaurand, P.; Schwartz, S. A.; Billheimer, D.; Xu, B. J.; Crecelius, A.; Caprioli, R. M. *Anal. Chem.* **2004**, *76*, 1145−1155.
(9) Preisler, J.; Hu, P.; Rejtar, T.; Moskovets, E.; Karger, B. L. *Anal. Chem.* **2002**, *74*, 17−25.
(10) Rohner, T. C.; Staab, D.; Stoeckli, M. *Mech. Ageing. Dev.* **2005**, *126*, 177−185.
(11) Spraggins, J. M.; Caprioli, R. M. *J. Am. Soc. Mass Spectrom.* **2011**, *22*, 1022−1031.
(12) Sherrod, S. D.; Castellana, E. T.; McLean, J. A.; Russell, D. H. *Int. J. Mass Spectrom.* **2007**, *262*, 256−262.
(13) Jungmann, J. H.; Smith, D. F.; MacAleese, L.; Klinkert, I.; Visser, J.; Heeren, R. M.A. *J. Am. Soc. Mass Spectrom.* **2012**, *23*, 1679−1688.
(14) Moskovets, E.; Preisler, J.; Chen, H. S.; Rejtar, T.; Andreev, V.; Karger, B. L. *Anal. Chem.* **2006**, *78*, 912−919.
(15) Schramm, T.; Hester, A.; Klinkert, I.; Both, J. P.; Heeren, M. A. R.; Brunelle, A.; Laprévote, O.; Desbenoit, N.; Robbe, M. F.; Stoeckli, M.; Spengler, B.; Römpp, A. *J. Proteomics* **2012**, *75*, 5106−5110.
(16) Hillenkamp, F.; Karas, M.; Beavis, R. C.; Chait, B. T. *Anal. Chem.* **1991**, *63*, 1193A−1203A.